Enantiomeric Analysis of Pharmaceutical Compounds by Ion/Molecule Reactions

Gabriela Grigorean and Carlito B. Lebrilla*

Department of Chemistry, University of California, Davis, California 95616

Protonated complexes involving cyclodextrin hosts and guest compounds that are pharmacologically important are produced in the gas phase and reacted with a gaseous amine. The guest is exchanged to produce a new protonated complex with the amine. The reaction is enantioselective and is used to develop a method for determining enantiomeric excess using only mass spectrometry. The pharmaceutical compounds include DOPA, amphetamine, ephedrine, and penicillamine. The presence of more than one reacting species is observed with DOPA and penicillamine. Molecular dynamics calculations are used to understand the nature of the interactions and the possible source of the variations in the reactivities.

The determination of enantiomeric excess in mixtures of chiral drugs and pharmaceutically important compounds is commonly performed with high-performance liquid chromatography (HPLC)[1–3] and, increasingly, capillary electrophoresis (CE).[4,5] However, the determination of enantiomeric excess strictly by mass spectrometry has several potentially attractive features over existing techniques. The duty cycle is fast compared to chromatographic methods. A mass spectrometric method does not necessarily require derivatization and is capable of high sensitivities. Moreover, mass spectrometry provides structural confirmation that is important in the analysis of complex, heterogeneous mixtures.

Methods that employ mass spectrometry specifically for the analyses of enantiomers often require chiral coanalytes to produce stereomeric complexes that have either unique ionization efficiencies or unique fragmentation behavior. Coanalytes that have been used in this manner include, but have not been limited to, alkyl tartrates,[6–8] cyclodextrins,[9,10] proteins,[11,12] amino acids[13] and pep-

tides, and crown ethers.[14–20] The resulting complexes are diastereomeric with either unique ionization efficiencies or fragmentation patterns that allow enantioselectivity based on the relative abundances of the respective peaks. A recent example includes the chiral differentiation of amino acids by the collision-induced dissociation of protonated trimers composed of the amino acid and two selector molecules, which are derivatized amino acids (*N-tert*-butoxycarbonylphenylalanine, *N-tert*-butoxycarbonylproline, and N-*tert*-butoxycarbonyl-*O*-benzylserine).[21] The same method was used to quantify enantiomeric excess in mixtures.[22]
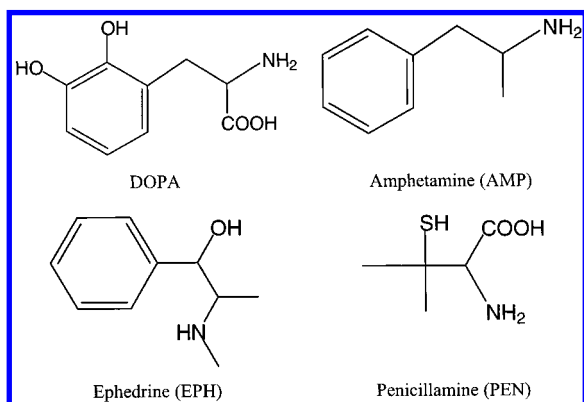
Metal complexes with chiral coanalytes have also been used to produce diastereomeric complexes that were probed by collision-induced dissociation. These analyses were performed by monitoring the relative abundances of the dissociation products that varied with the chirality of the analyte. Complexes of cobalt[23,24] and copper[25,26] have been used in this manner. Recent examples with the copper complexes show considerable promise as a method for quantification.[26]

Ion–molecule reactions in the gas phase provide an alternative method for chiral recognition and quantification. Enantioselectivity has been achieved with the use of crown ethers[19,20,27] and

(1) Gübitz, G. *Chromatographia* **1990**, *30,* 555–564.
(2) Ameyibor, E.; Stewart, J. T. *J. Liq. Chromatogr., Relat. Technol.* **1997**, *20,* 855–869.
(3) Tang, Y. *Chirality* **1996**, *8,* 136–142.
(4) Blaschke, G.; Chankvetadze, B. *J. Chromatogr., A* **2000**, *875,* 3–25.
(5) Fillet, M.; Hubert, P.; Crommen, J. *J. Chromatogr., A* **2000**, *875,* 123–134.
(6) Fales, H. M.; Wright, G. W. *J. Am. Chem. Soc.* **1977**, *99,* 2339–2340.
(7) Nikolaev, E. N.; Goginashvily, G. T.; Talrose, V. L.; Kostjanovsky, R. G. *Int. J. Mass Spectrom. Ion Processes* **1988**, *86,* 249–252.
(8) Denisov, E. N.; Shustryakov, V.; Nikolaev, E. N.; Winkler, F. J.; Medina, R. *Int. J. Mass Spectrom. Ion Processes* **1999**, *183,* 357–368.
(9) Ramirez, J.; He, F.; Lebrilla, C. B. *J. Am. Chem. Soc.* **1998**, *120,* 7387–7388.
(10) Grigorean, G.; Ramirez, J.; Ahn, S. H.; Lebrilla, C. B. *Anal. Chem.* **2000**, *72,* 4275–4281.
(11) Camara, E.; Green, M. K.; Penn, S. G.; Lebrilla, C. B. *J. Am. Chem. Soc.* **1996**, *118,* 8751–8752.

(12) Gong, S.; Camara, E.; He, F.; Green, M. K.; Lebrilla, C. B. *Int. J. Mass Spectrom. Ion Processes* **1999**, *185/186/187,* 401–412.
(13) Vekey, K.; Czira, G. *Anal. Chem.* **1997**, *69,* 1700–1705.
(14) Sawada, M.; Takai, Y.; Yamada, H.; Kaneda, T.; Kamada, K.; Mizooku, T.; Hirose, K.; Tobe, Y.; Naemura, K. *Chem. Commun.* **1994**, 2497–2498.
(15) Sawada, M.; Okumura, Y.; Yamada, H.; Takai, Y.; Takahashi, S.; Kaneda, T.; Hirose, K.; Misumi, S. *Org. Mass Spectrom.* **1993**, *28,* 1525–1528.
(16) Sawada, M.; Takai, Y.; Yamada, H.; Hirayama, S.; Kaneda, T.; Tanaka, T.; Kamada, K.; Mizooku, T.; Takeuchi, S.; Ueno, K.; Hirose, K.; Tobe, Y.; Naemura, K. *J. Am. Chem. Soc.* **1995**, *117,* 7726–7736.
(17) Sawada, M.; Okumura, Y.; Shizuma, M.; Takai, Y.; Hidaka, Y.; Yamada, H.; Tanaka, T.; Kaneda, T.; Hirose, K.; Misumi, S.; Takashi, S. *J. Am. Chem. Soc.* **1993**, *115,* 7381–7388.
(18) Sawada, M.; Shizuma, M.; Takai, Y.; Yamada, H.; Kaneda, T.; Hanafusa, T. *J. Am. Chem. Soc.* **1992**, *114,* 4405–4406.
(19) Chu, I. H.; Dearden, D. V.; Bradshaw, J. S.; Huszthy, P.; Izatt, R. M. *J. Am. Chem. Soc.* **1993**, *115,* 4318–4320.
(20) Dearden, D. V.; Dejsupa, C.; Liang, Y. J.; Bradshaw, J. S.; Izatt, R. M. *J. Am. Chem. Soc.* **1997**, *119,* 353–359.
(21) Yao, Z. P.; Wan, T. S. M.; Kwong, K. P.; Che, C. T. *Anal. Chem.* **2000**, *72,* 5383–5393.
(22) Yao, Z. P.; Wan, T. S. M.; Kwong, K. P.; Che, C. T. *Anal. Chem.* **2000**, *72,* 5394–5401.
(23) Hofmeister, G.; Leary, J. A. *Org. Mass Spectrom.* **1991**, *26,* 811–812.
(24) Dang, T. T.; Pedersen, S. F.; Leary, J. A. *J. Am. Soc. Mass Spectrom.* **1994**, *5,* 452–459.
(25) Tao, W. A.; Zhang, D.; Wang, F.; Thomas, P. D.; Cooks, R. G. *Anal. Chem.* **1999**, *71,* 4427–4429.
(26) Tao, W. A.; Zhang, D.; Nikolaev, E. N.; Cooks, R. G. *J. Am. Chem. Soc.* **2000**, *122,* 10598–10609.
(27) Liang, Y.; Bradshaw, J. S.; Izatt, R. M.; Pope, R. M.; Dearden, D. V. *Int. J. Mass Spectrom.* **1999**, *185/186/187,* 977–988.

Chart 1. Pharmaceutically Active Compounds Used for Enantioselective Guest Exchange Reactions

cyclodextrins.[9] In this report, an enantiomeric analysis method is developed based on the differences in the reaction rates of gas-phase host−guest complexes. A diastereomeric complex [HO:A + H]$^+$ of an oligosaccharide host (HO) with a chiral analyte guest (A) reacts with an alkylamine (B) to produce a guest exchange product ([HO:B + H]$^+$) illustrated in reaction 1.

$$[HO:A + H]^+ + B \rightleftharpoons [HO:B + H]^+ + A \qquad (1)$$

The reaction is effectively a proton-transfer process mediated by a host molecule. This reaction has been studied extensively with amino acids.[28] The "three-point interaction" construct was used to understand the nature of the enantioselectivity. It has also been shown that the formation of gas-phase inclusion complexes plays a prominent role in the reaction.[29] In this report, we expand this work and illustrate that the same reaction can be used to develop a method for enantiomeric determinations of pharmaceutical compounds.

Four commonly used chiral drugs were examined: L- and D-DOPA, l- and d-amphetamine (AMP), l- and d-ephedrine (EPH), and L- and D-penicillamine (PEN) (Chart 1). DOPA in the l-form is used for the treatment of Parkinson's disease. Amphetamine in the l-form is a central nervous system stimulant. Ephedrine, also in the l-form, is used as brochodilator and its derivative, pseudoephedrine, is a decongestant in the d-form. Penicillamine is used as an antirheumatic. All have a single chiral center except for the ephedrine, which has two.

EXPERIMENTAL SECTION

Materials. The pharmaceutical analytes 3,4-dihydroxyphenyl-alanine (DOPA), amphetamine, and ephedrine were purchased from Sigma Chemical Co. (St. Louis, MO). Penicillamine was purchased from Aldrich (Milwaukee, WI). All were used without further purification. The hosts employed were permethylated β-cyclodextrin (heptakis(2,3,6-tri-*O*-methyl)-β-cyclodextrin or CD), purchased from Sigma, and permethylated maltoheptaose (or HEP), synthesized in this laboratory from the parent (Sigma) via

the method of Ciucanu and Kerek.[30] All alkylamines used in the study including *n*-propylamine, (*R*)-1-amino-2-propanol, ethylene-diamine, and 1,3-diaminopropane were obtained from Aldrich.

Exchange Reactions. All the experiments were performed on a home-built external source electrospray FTMS instrument equipped with a 5.2-T superconducting magnet described in earlier publications.[28,31] The hosts and analytes were dissolved in a 1:1 H$_2$O/MeOH solution. The complexes were then prepared by mixing the 0.01 M host solution with the 0.01 M drug analyte solution, in a 1:100 ratio, respectively. To introduce solution into the FTMS, a microspray setup was used. The solution was pumped through a stainless steel tube, 0.02 in. i.d., 3 in. long, attached to a Hamilton syringe on one end and the capillary needle at the other end. The needle was made of fused-silica capillary tubing, 25 μm i.d., 150 μm O.D. The flow rate used was 12 μL/h. A voltage of 1.5−2.5 kV was applied to create the charged spray, which then drifted into a heated stainless steel capillary inside the source. The alkylamine was purified in the vacuum manifold with several freeze−thaw cycles. It was introduced into the analyzer chamber using a variable leak valve. The pressure of the amine was between 1 × 10^{-7} and 6 × 10^{-7} Torr. Although attempts were made to calibrate the ion gauge using efficiency factors,[32] large variations between the "true" pressure and the recorded pressures are expected. The variation in the pressures is the source of most of the error in the absolute rate constants. Although these errors cancel in the selectivity values, it is suggested that the absolute rates are treated as those obtained from an uncalibrated ion gauge.

To obtain the rate constants, the reactant [HO:A + H]$^+$ and product [HO:B + H]$^+$ peaks were monitored as a function of time. Several rf bursts were used to eliminate unwanted masses such as those belonging to complexes of Na$^+$ and K$^+$ along with any residual [HO:B + H]$^+$ peaks present at the beginning of the exchange reaction.

Molecular Modeling. The cyclodextrin and the protonated analyte structures were constructed and separately optimized fully using the Insight II builder module. The protonated oligosaccha-ride−analyte complexes were then formed by merging the respective oligosaccharide hosts and the analyte guests. Two sets of calculations were performed corresponding to two types of initial structures. In one set, the analytes were placed inside the cavity to produce initially inclusion complexes. In a second set, the analytes were placed on the outer wall of the host. In both cases, calculations of the complexes were started with fully optimized oligosaccharide host and amino acid structures. During the simulation, the structures of both the analytes and the hosts were allowed to fully optimize. The simulation was performed by heating the complexes to 600 K for 400 ps. At 8-ps intervals, a structure from the trajectory was captured and annealed in steps of 100 K to 0 K. This resulted in 50 annealing simulations with a corresponding number of structures. Although only one structure is shown in each case, all the structures within 5 kcal/mol of the lowest energy structure were examined. Unless indicated, these structures were found to share the same structural features as the lowest.

(28) Ahn, S.; Ramirez, J.; Grigorean, G.; Lebrilla, C. B. *J. Am. Soc. Mass Spectrom.*, in press.

(29) Ramirez, J.; Ahn, S.; Grigorean, G.; Lebrilla, C. B. *J. Am. Chem. Soc.* **2000**, *122*, 6884−6890.

(30) Ciucanu, I.; Kerek, F. *Carbohydr. Res.* **1984**, *131*, 209−217.

(31) Carroll, J. A.; Penn, S. G.; Fannin, S. T.; Wu, J.; Cancilla, M. T.; Green, M. K.; Lebrilla, C. B. *Anal. Chem.* **1996**, *68*, 1798−1804.

(32) Bartmess, J. E.; Georgiadis, R. M. *Vacuum* **1983**, *33*, 149−153.

Table 1. Selectivities for the CD Host ($k \times 10^{-11} \text{cm}^3/\text{molecule·s}$)

	n-propyl-amine	(R)-1-amino-2-propanol	ethylene-diamine	1,3-diamino-propane
		DOPA		
k_L	$<10^{-15}$	0.0047	0.0121	fast: 0.122 slow: 0.031
k_D	$<10^{-15}$	$<10^{-15}$	0.0024	fast: 0.131 slow: 0.014
k_L/k_D			4.98	fast: 0.93 slow: 2.19
		Amphetamine		
k_l	0.40	1.78		
k_d	0.27	1.34		
k_l/k_d	1.46	1.33		
		Ephedrine		
$k_{(+)}$	0.031	0.53		
$k_{(-)}$		0.64		
$k_{(+)}/k_{(-)}$		0.83		
		Penicillamine		
k_L	3.4			
k_D	fast: 1.80 slow: 0.55			
k_L/k_D	fast: 1.9 slow: 6.18			

Table 2. Selectivities for the HEP Host ($k \times 10^{-11} \text{cm}^3/\text{molecule·s}$)

	n-propyl-amine	$(R)-1$-amino-2-propanol	ethylene-diamine	1,3-diamino-propane
		DOPA		
k_L	$<10^{-15}$		0.00982	
k_D	$<10^{-15}$		0.00805	
k_L/k_D			1.22	
		Amphetamine		
k_l	2.22			
k_d	2.47			
k_l/k_d	0.90			
		Ephedrine		
$k_{(+)}$		1.58		
$k_{(-)}$		2.02		
$k_{(+)}/k_{(-)}$		0.78		
		Penicillamine		
k_L	4.48			
k_D	fast: 4.15 slow: 0.42			
k_L/k_D	fast: 1.07 slow: 1.85			

RESULTS

A. Rate Constants. Enantioselectivity (S) is defined in this discussion by the ratio of the rate constants ($S = k_L/k_D$). For convenience, both L and l, and similarly D and d, will be grouped together in defining selectivity, with the understanding that the nature of the two sets of nomenclatures is significantly different. An S value of 1.0 indicates no chiral differentiation between the enantiomers in question. For the amino acids reported in previous studies, the values were as large as 5.[9,28,29] In some cases, the ratios were less than 1, which indicated that the D-enantiomers were favored. It is not yet possible to predict which enantiomer will be favored in the guest-exchange reaction, albeit for the amino acids the L typically gave the largest rate constants.[9,29] Molecular modeling calculations give qualitative indications when the selectivity or its inverse will be large based on differences in the interaction between the host and the guest. However, molecular modeling also cannot yet be used to predict whether the selectivity is greater or less than unity. Tables 1 and 2 list the selectivities of the drugs discussed in this paper.

Amphetamine. To obtain the rate constants, the relative intensities of each pure enantiomer were monitored throughout an appropriate length of the reaction period. Figure 1 illustrates the mass spectra of the reaction mixture at various reacting times. The series of mass spectra in Figure 1 reflect the differences in reaction rates for the l- (left spectra) and d- (right) forms of amphetamine. Time zero was set to the end of the ejection pulse that eliminated the product peak [CD:NPA + H]$^+$ resulting from the initial reaction of the drug complex. Therefore, the mass spectrum at time zero contained primarily the complex ion [CD:AMP + H]$^+$. As the reaction progressed from 9 to 49 s, the [CD:AMP + H]$^+$ reactant peak (m/z 1565) decreased; the rate of this decrease differed between the l- and d-forms, with the latter having its reactant peak exhausted at a slower rate. When the reactant peak was exhausted to an intensity of ~5% of the product peak, data collection was stopped to ensure accuracy of the intensity values.
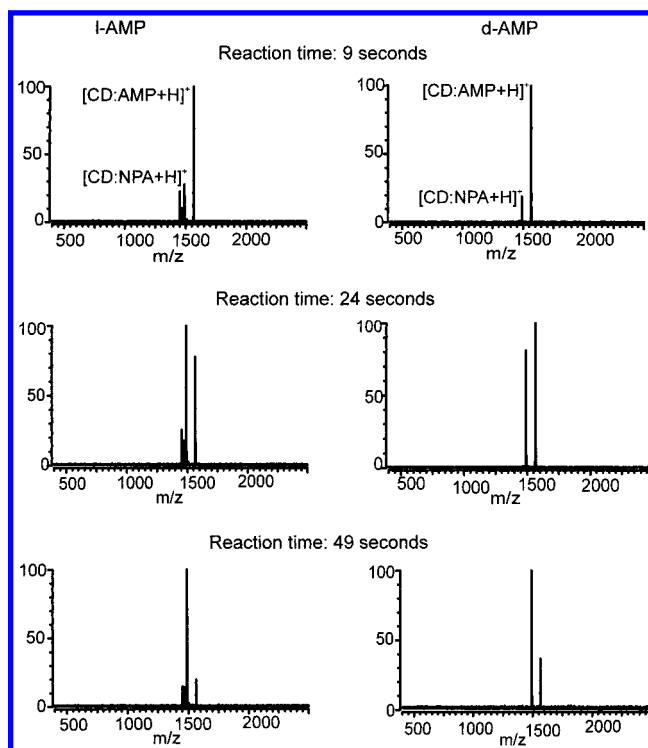

Figure 1. ESI-FTMS spectra of a solution containing β-cyclodextrin and amphetamines at various reaction times. The complex [CD: Amp+H]$^+$ is isolated and allowed to react with a background pressure of n-propylamine of 3.2×10^{-7} Torr. This reaction has a relatively low selectivity corresponding to $S = 1.46$.

A rate plot for the protonated amphetamine−cyclodextrin complex [CD:AMP + H]$^+$ reacting with n-propylamine is shown in Figure 2. For both plots, $r^2 = 0.999$. From the rate curves, the rate constants for the two enantiomers were found to be $k_L = 0.40 \times 10^{-11}$ cm^3/molecule·s and $k_D = 0.27 \times 10^{-11}$cm^3/molecule·s giving a selectivity $S = 1.46$.

The selectivities of this compound was further examined with other bases and other host molecules. When a more basic compound was used for the exchange reaction, such as 1-amino-
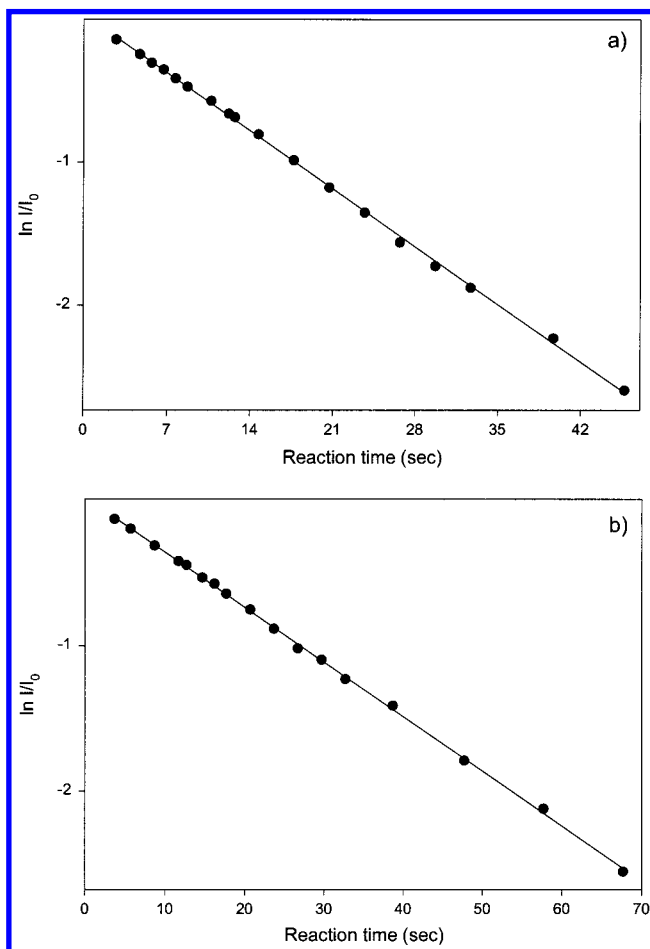
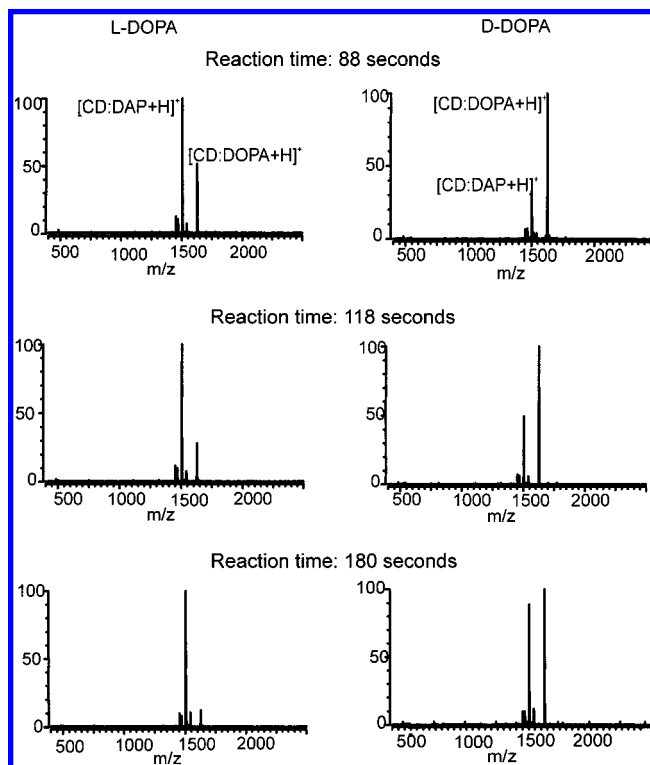**Figure 2.** Rate plot of the reaction illustrated in Figure 1. For both enantiomers, $r^2 = 0.999$. (a) d-AMP. (b) l-AMP.

Figure 3. ESI-FTMS spectra under three reaction times of a solution containing β-cyclodextrin and DOPA. The complex [CD:DOPA+H]$^+$ is reacted with 1,3-diaminopropane (DAP) (4.0×10^{-7} Torr).

2-propanol, the reactivity of both isomers increased but the selectivity decreased to 1.33. The selectivity reversed when a linear oligosaccharide (permethylated maltoheptaose or HEP) was used as host (Table 2).

DOPA. The addition of the hydroxyl group on the phenyl rings significantly decreased the rate of exchange for DOPA. Exchange reactions performed with the monoamine bases n-propylamine and 1-amino-2-propanol were extremely slow compared to phenylalanine ($k = 10^{-11}$ cm^3/molecule·s[29]). The reaction of the [CD:DOPA+H]$^+$ complex with n-propylamine was not conducive to obtaining the reaction rate constants indicating that the rate constants were less than 10^{-15} cm^3/molecule·s. For the reaction of the complex with 1-amino-2-propanol, only the l-form of the drug exchanged within a time frame where obtaining the reaction rate constant was still feasible, with $k_L = 0.47 \times 10^{-13}$ cm^3/molecule·s. Not surprisingly, gas-phase basicity played a role in the rate of the gas-phase exchange reaction. For this reason, more basic compounds such as the diamines like 1,3-diaminopropane (GB 987 versus 889 kJ/mol for n-propylamine) were used for the guest exchange reactions.

The reactions of the complexes of DOPA [CD:DOPA+H]$^+$ and [HEP:DOPA+H]$^+$ with ethylenediamine yielded the usual linear rate plots with r^2 values of 0.999 (data not shown). The reactivity of the l-isomer was nearly of the same magnitude for both hosts; the exchange reaction rate is $k_L = 1.21 \times 10^{-13}$ cm^3/molecule·s for the CD host and $k_L = 0.98 \times 10^{-13}$ cm^3/molecule·s for the

HEP host. The selectivities varied considerably between the two hosts with a value of 5.0 for CD and 1.22 for HEP. These values contrast to the selectivity of the phenylalanine, which exhibited a higher selectivity with the linear HEP host (4.6) than with the CD host (0.83).

The series of mass spectra in Figure 3 from the reaction of 1,3-diaminopropane and [CD:DOPA+H]$^+$ illustrate the spectral features of an analyte with relatively large selectivities. The resulting kinetic plot yielded a break in the curve suggesting the presence of at least two reactive species in the ion population (Figure 4). Both the l- and the d-forms have fast and slow components that differed by an order of magnitude. For example, the l-form has values of $k_{L,fast} = 12.2 \times 10^{-13}$ cm^3/molecule·s and $k_{L,slow} = 3.1 \times 10^{-13}$ cm^3/molecule·s.

Ephedrine. This compound provides a good contrast to the others because it has two chiral centers. Exchange reactions with 1-amino-2-propanol were performed with both hosts, CD and HEP. The kinetic plots showed the usual linear behavior with rate constants that are slightly slower than amphetamine. However, increasing the number of chiral centers did not apparently increase the selectivity; poor enantioselectivities were obtained with values close to 1. For the host β-CD, S equaled 0.83 and for HEP, S equaled 0.78.

Penicillamine. The complex undergoes relatively fast exchanges, even faster than amphetamine. The kinetic plot of the complex yielded the usual straight line for the l-isomer, but the d-isomer showed the two-component behavior when the complex [CD:PEN+H]$^+$ was reacted with n-propylamine (Figure 5a). The l-enantiomer of the drug has a rate constant $k_L = 3.40 \times 10^{-11}$. The d-enantiomer displayed a two-component curve, with $k_{D,fast} = 1.88 \times 10^{-11}$ and $k_{D,slow} = 0.55 \times 10^{-11}$ (Figure 5b). This behavior
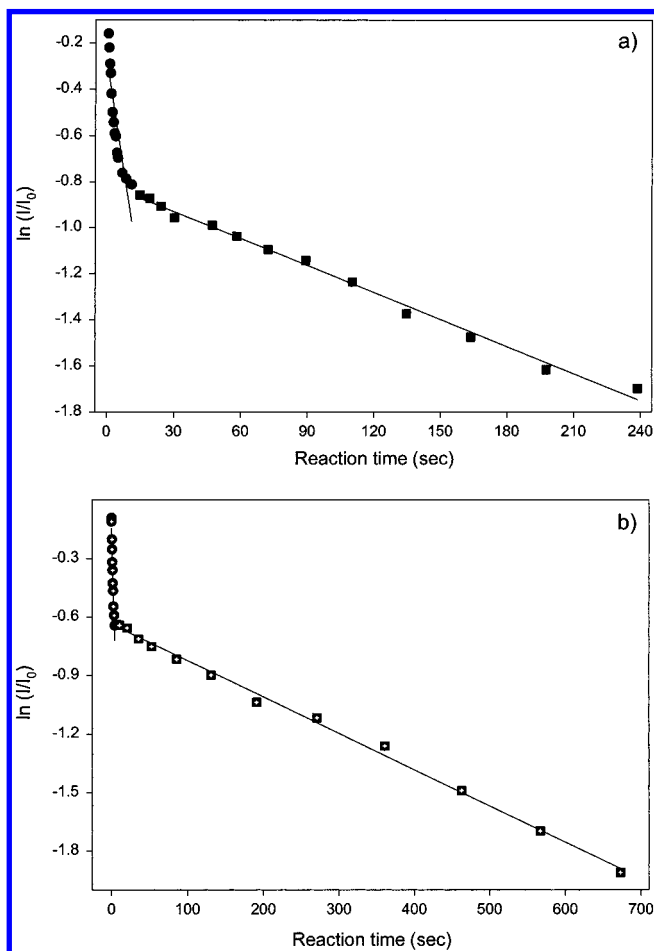
Figure 4. Kinetic plot for the reaction of 1,3-diaminopropane with [CD:DOPA+H]$^+$ (Figure 3). Both enantiomers have at least two reactive components, fast and slow. The rate constant of the slow reaction is significantly smaller than the fast reaction. (a) L-DOPA. (b) D-DOPA.

Figure 5. Rate plots for the reaction of protonated penicillamine complexed to β-cyclodextrin with n-propylamine. The L-enantiomer has a linear behavior while the D-enantiomer shows a break in the plot corresponding to two reacting species. (a) L-PEN. (b) D-PEN.

is unique and is not observed with any other pharmaceutical compounds or with the amino acids. It suggests not only differences in the interactions between each enantiomer and the host but also that the D-enantiomer may interact with the host to produce two distinct complexes with different reactivities. The ratio $k_L/k_{D,fast} = 1.9$, which is similar to the 2.2 value for cysteine—its structural analogue. The ratio involving the slow reaction is even larger with $k_L/k_{D,slow} = 6.2$.

B. Quantitative Analyses of Chiral Drugs by Mass Spectrometry. To illustrate the analytical application of the guest exchange reaction to pharmaceutical compounds, calibration curves were constructed. To construct calibration curves, a known set of enantiomeric mixtures is analyzed, beginning with the one pure enantiomer and ending with the other. The procedure involves first choosing the proper conditions for the exchange reaction. Parameters include the alkylamine reagent, its pressure, and a reaction time. The optimum reaction time for analysis is the shortest reaction period that produces a spectrum with sufficiently large differences in relative intensities. A known analyte is then analyzed in the following manner. The enantiomeric composition of the known analyte is varied, beginning with one pure component (100:0) to include several compositions such as 80:20, 65:35, 50:50, 35:65, 20:80, and 0:100. Mass spectra for these
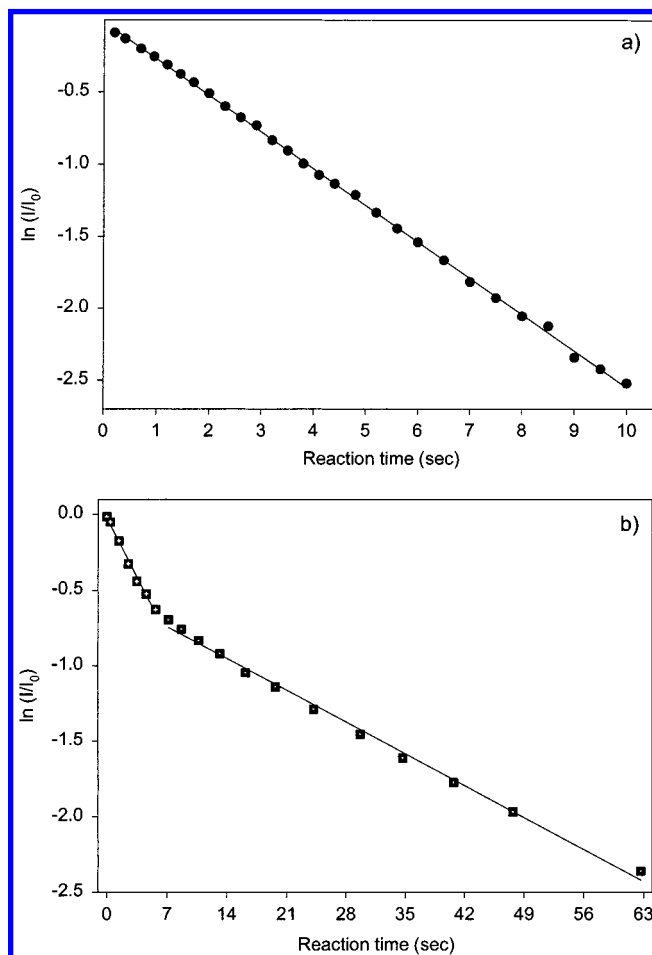
mixtures are obtained at the chosen reaction time. We have looked at the reaction rates as the enantiomer composition changed, and as expected, the combined reaction rate increases as the percentage of the slower enantiomer increases in the analyte mixture. From the mass spectra, a calibration curve is constructed. The plot has as the ordinate I/I_0, with I as product peak and I_0 the sum of the reactant peak intensity and product peak intensity. The abscissa is D/(D + L), the D-enantiomer mole fraction.

The quality of the calibration curve is dependent on the selectivity value, with larger scatter, hence largest error, as S approaches unity. For example, Figure 6 shows a curve for amphetamine with an r^2 value of 0.971. To produce this curve, n-propylamine was used as the reagent gas and cyclodextrin was used as the host with a reaction time of 39 s. The selectivity of this system was $S = 1.46$.

With a larger selectivity value of 2.19 (cyclodextrin host and 1,3-diaminopropane as reagent gas) DOPA yielded $r^2 = 0.996$ (Figure 7). To produce this calibration curve, a reaction time of 88 s was used. Apparently, even with two reacting species it is possible to construct a valid calibration curve.

DISCUSSION

Chiral differentiation in the gas phase is governed by the three-point interaction. This model, illustrated in Chart 2, requires three
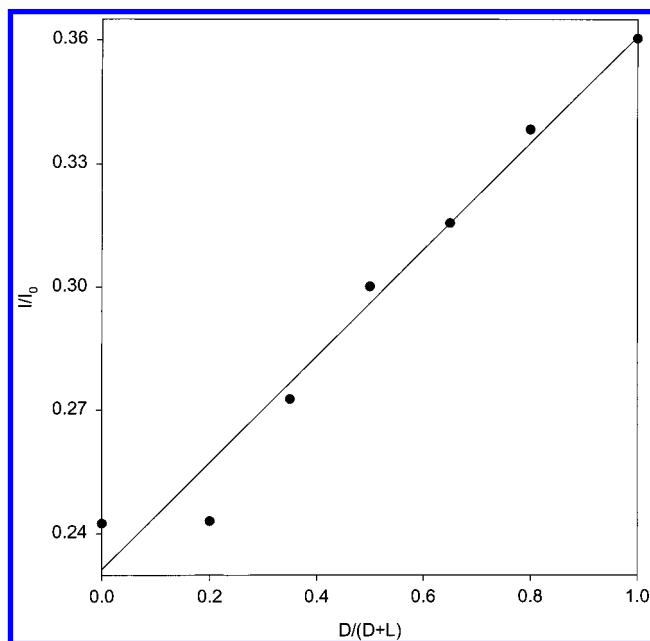
Figure 6. Calibration curve for a compound, amphetamine, with a low selectivity ($S = 1.46$). The reactant complex is composed of protonated amphetamine and β-cyclodextrin and reacted with n-propylamine. The value of r^2 is 0.971.
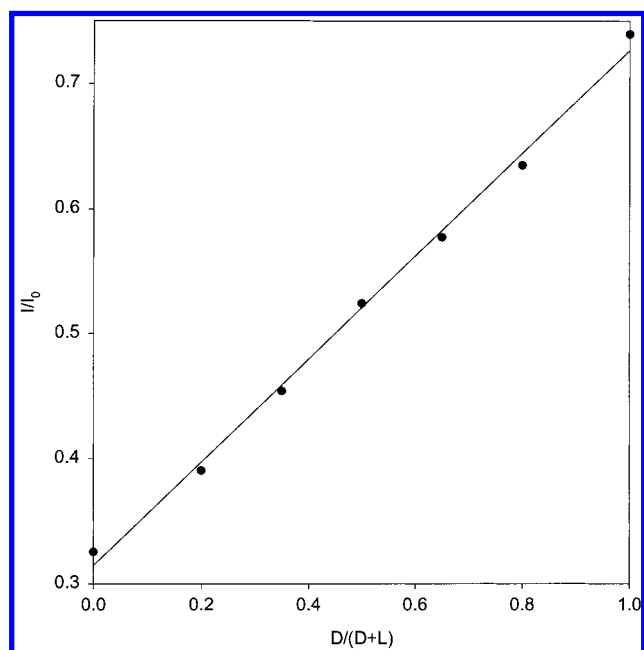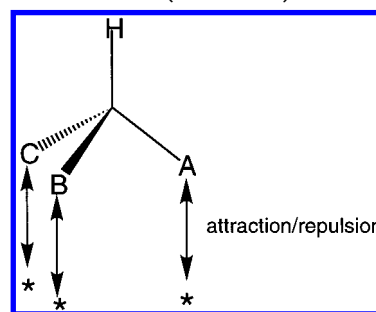

Figure 7. Calibration curve for a compound with moderate selectivity (2.19). The reactant complex, protonated DOPA and β-cyclodextrin, is reacted with 1,3-diaminopropane. The value of r^2 is 0.996.

interacting points between the host and the guest as the prerequisite for enantioselectivity. Although this construct is commonly used in the solution phase, its application in the gas phase to predict the extent of enantioselectivity has recently been reported.[28]

The low selectivity of amphetamine is explained by the three-point interaction. In the gas-phase complex, amphetamine is protonated on the amine group. The ammonium group interacts positively with the methoxyl groups, specifically the narrow rim, which is composed of the carbon-6 of glucose. The molecular modeling performed on the protonated complex [CD:AMP+H]$^+$

Chart 2. Three-Point Interaction Involving the Analyte and the Host (Asterisk)

illustrates the nature of the interaction (Figure 8). Both enanti-omers interact similarly with the ammonium interacting with the lower rim while the phenyl group is constrained by the inner cavity. This interaction represents the second interaction while the interaction of the methyl with the inner cavity represents the third. Thus, amphetamine has a single attractive interaction and two steric or repulsive interactions. Studies with amino acids indicate that two attractive interactions provide the largest selectivity while three and one attractive interactions decrease the selectivity.[28]

The guest exchange reaction of DOPA is unique for several reasons. The reaction is extremely slow, compared to compounds with similar structures such as tyrosine,[28,29] requiring strongly basic amines to perform the exchange reaction. The chiral selectivity is large, with the cyclodextrin host compared to structural analogues such as tyrosine ($S = 0.67$) and phenylalanine ($S = 0.82$).[10] The two rate constants for each enantiomer further suggest at least two reacting species. In the complex, this may be inferred as two species in which the analyte interacts with the host by different arrangements. DOPA effectively interacts with three points of attraction. Ion/dipole and hydrogen-bonding interactions occur with the protonated ammonium group. The carboxylic acid and the hydroxyl groups on the phenyl undergo hydrogen-bonding interactions. Studies with amino acids such as threonine and methionine indicate that a three-point attraction does not necessarily increase the selectivity.[29] The results of the molecular modeling of the DOPA complex are summarized in Figure 9. The upper structures are the result of calculations where the initial structures involved inclusion of the analyte. The two lower structures were initiated with the DOPA near the outer wall of the cyclodextrin cavity. The results indicate that molecule migrates into the cyclodextrin during the annealing cycles and further suggest that inclusion is the preferred state of interaction.[29]

The upper structures in Figure 9 are similar in appearance. The carboxylic and the ammonium groups in both enantiomers interact with the lower rim. Both functional groups are constrained by the phenyl group, which in turn is constrained by the cavity. We also find that the hydroxyl group interacts with the upper rim. The similarities in the interaction of the two enantiomers were also observed with Phe and Tyr, both of which have low selectivities. We posit that these structures represent the fast-reacting components as these are predicted to have low selectivi-ties ($S_{fast} = 0.93$) (Table 1). The other structures (lower) exhibit large differences in their interactions and may represent the slowly reacting components, which have a larger selectivity ($S_{slow} = 2.19$).

Ephedrine contains two chiral centers, but the presence of a second chiral center does not apparently increase selectivity. The
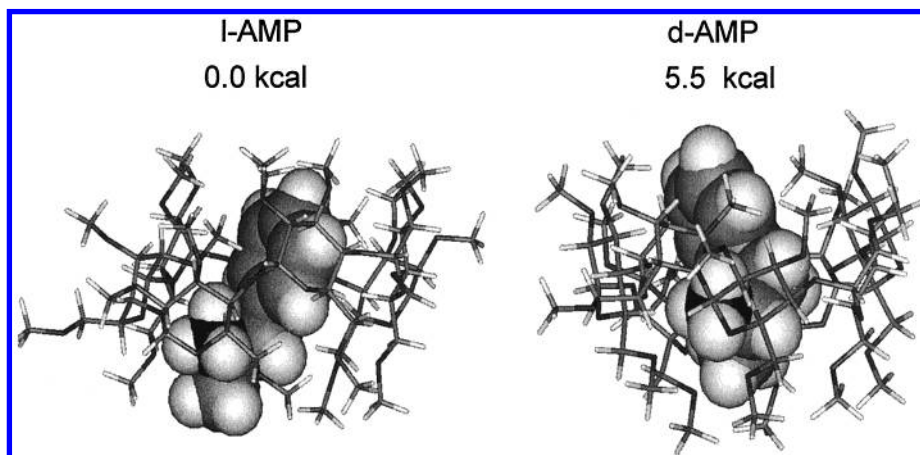
Figure 8. Lowest energy structures produced by molecular modeling of the complex [CD:AMP+H]$^+$. The *l*-enantiomer is shown on the left. The heat of formation (kcal/mol) is relative to the lowest energy structure.
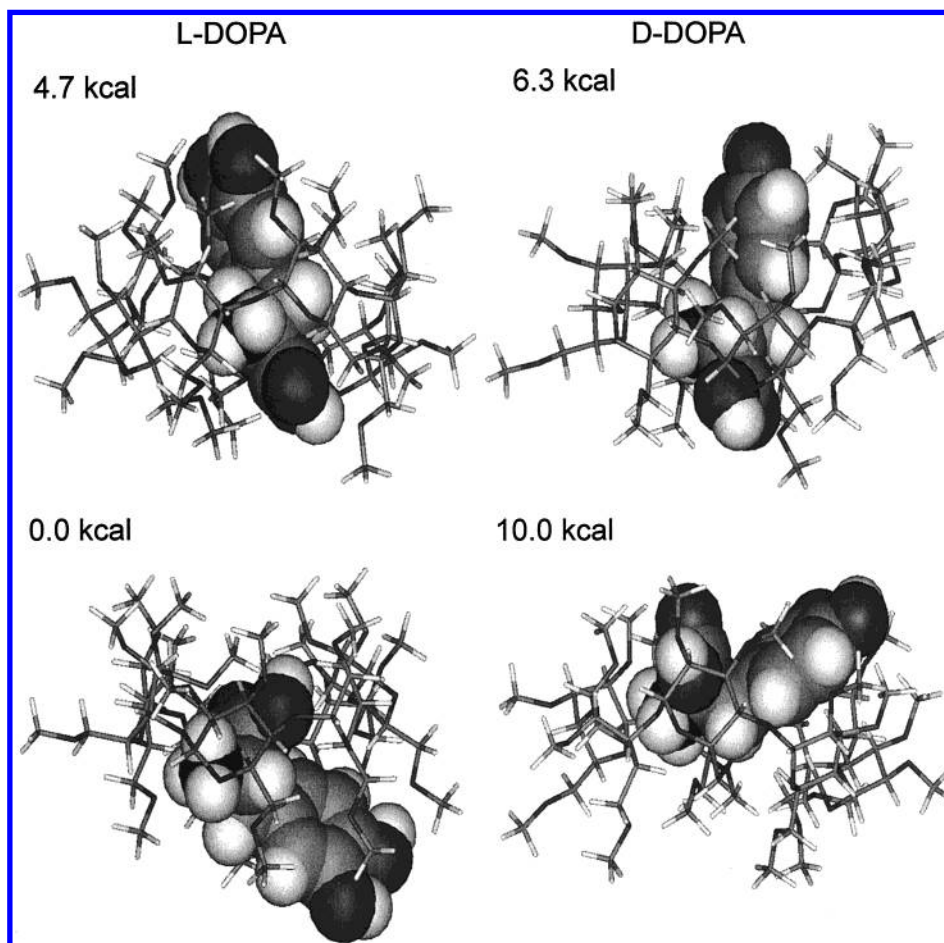

Figure 9. Lowest energy structures produced by molecular modeling of the complex [CD:DOPA+H]$^+$. The two top structures were the results of calculations where the initial geometry was the inclusion complex. The two bottom structures were initiated with the analyte on the outer cavity of the host.

selectivity of ephedrine is poor with both CD ($S = 0.83$) and HEP ($S = 0.78$). Taking into account the interactions of the protonated analyte with the host, we find one attraction due to the protonated amine. However, this attraction may be sterically weakened because the group is a secondary amine. Similarly, the second attractive interaction due to the hydroxyl may also be attenuated by the presence of the bulky phenyl group. The third interaction is repulsive due to the methyl group. The number of net attractive

interactions is between one and two, which would be expected to yield poor enantioselectivity.

Penicillamine exhibits good selectivity because it has two strong attractive interactions. The S−H group is not expected to interact strongly with the ether groups on the host. The presence of two reacting species, as evidenced by the break in the kinetic plot of the cyclodextrin complex ([CD:PEN+H]$^+$) reacting with *n*-propylamine, is present but only for the D-enantiomer. The
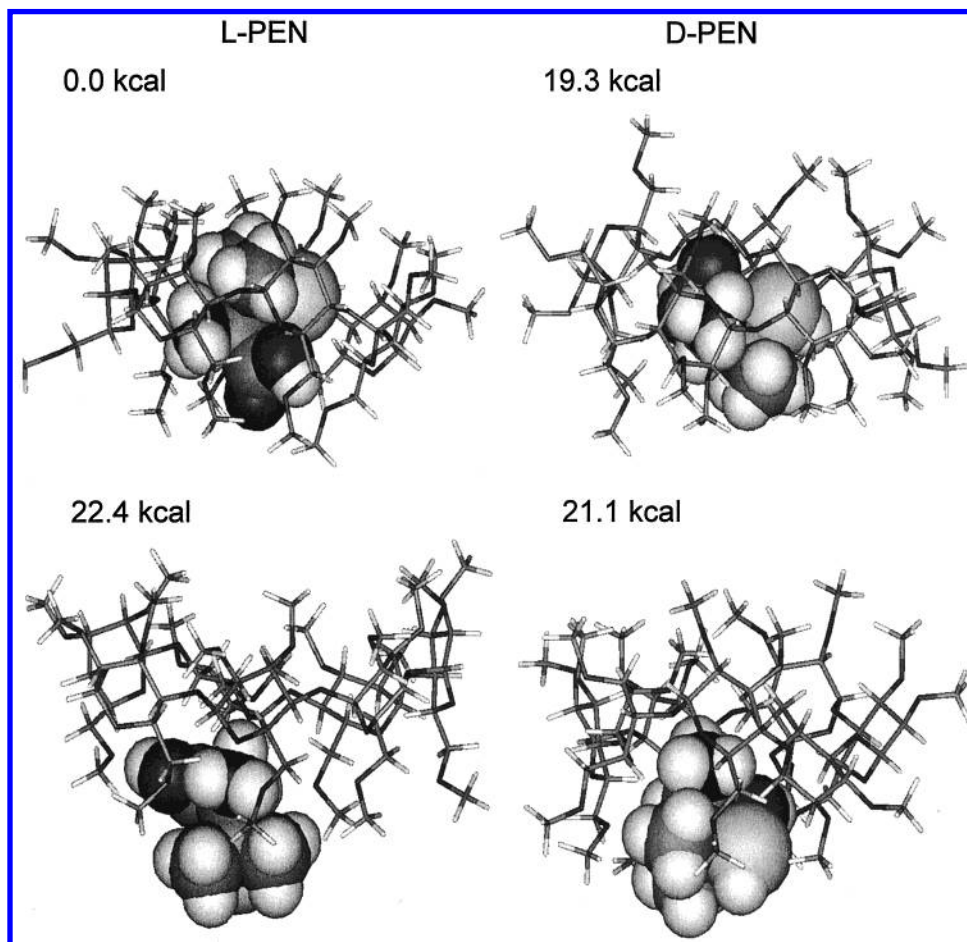
Figure 10. Lowest energy structures produced by molecular modeling of the complex [CD:PEN+H]$^+$. The two top structures were the results of calculations where the initial geometry was the inclusion complex. The two bottom structures were initiated with the analyte on the outer cavity of the host.

molecular modeling results are summarized in Figure 10 with the four most stable structures of the penicillamine complex beginning with the included structure (upper structures) and the noninincluded structures (lower). The D-isomer shows two structures with similar energies but with one fully included and the other partially included with the molecule protruding through the lower rim. The L-isomer yields two structures, but the inclusion complex is significantly more stable than the noninclusion structure. We posit that the high-energy structure converts to the low-energy structure during ionization so that only a single species is observed for the L-form while two species are observed for the D-form.

CONCLUSION

The determination of enantiomeric excess by employing ion/ molecule reactions and strictly mass spectrometry is illustrated.

The prerequisite for this method is that the analyte contains an amine. The interaction of the ammonium group with the host provides the stability for observing the host−guest complex in the gas phase. As with the amino acids, we find that the formation of inclusion complex is highly favorable and the complex is the most stable gas-phase species.